

4.2. Mixing of Liquids of Equal Viscosities and Densities.

Experiments were performed with solutions having the same viscosity and density, for different feeding rates. Compositions of these solutions are presented in table 4.I. Flow rates, mean velocities and Reynolds numbers for: dosing pipe (Q_1 , \bar{w}_1 , $Re_1 = \bar{w}_1 \cdot d_1 \cdot \rho / \mu$), the annular inlet (Q_2 , \bar{w}_2) and the cylindrical outlet section of the nozzle (\bar{w}_{out} , $Re_{out} = \bar{w}_{out} \cdot d_{out} \cdot \rho / \mu$) are shown in table 4.II. In all cases the flows in the dosing pipe and the mixer nozzle were laminar.

Table 4.I. Compositions and properties of the test solutions.

liquid	starch syrup [weight %]	I ₂ [mol/dm ³]	Na ₂ S ₂ O ₃ [mol/dm ³]	μ [Pa·s]	ρ [g/cm ³]
A	64.54	0.0251	0.0	0.0431	1.249
B	64.54	0.0	0.0106	0.0431	1.249

Table 4.II. Flow rates, mean velocities and Reynolds numbers.

exp. no.	Q_1 [cm ³ /s]	\bar{w}_1 [cm/s]	Re_1	Q_2 [cm ³ /s]	\bar{w}_2 [cm/s]	Q_2/Q_1	\bar{w}_{out} [cm/s]	Re_{out}
1	0.0928	4.341	2.075	9.899	0.7928	106.6	79.51	92.17
2	0.1997	9.339	4.466	9.846	0.7886	49.30	79.94	92.66
3	0.4197	19.63	9.385	9.352	0.7490	22.28	77.76	90.14
4	0.9868	46.15	22.07	8.926	0.7149	9.045	78.88	91.44

Analysis of the photographs shot during the experiments (figures 4.3abcd) indicates that the central iodine stream expands just behind the tip of the dosing pipe; the magnitude of the expansion depends on the flow inlet ratio Q_2/Q_1 . In the cylindrical part of the mixer a core-annular flow is well observed. The contraction of the iodine stream is visible in the cone-shaped stretching section of the mixer.

In all cases the central stream was stable; no deflection from the mixer axis and no propagation of disturbances were detected. A closer inspection of the photographs reveals also no significant influence of molecular diffusion and chemical reaction between iodine and sodium thiosulfate on the shape of coloured zone. The boundary between the core and the annular streams was always sharp and easily detectable. A good agreement was found between the experimental shape of the iodine streams and the calculated concentration contours of the reacting species.

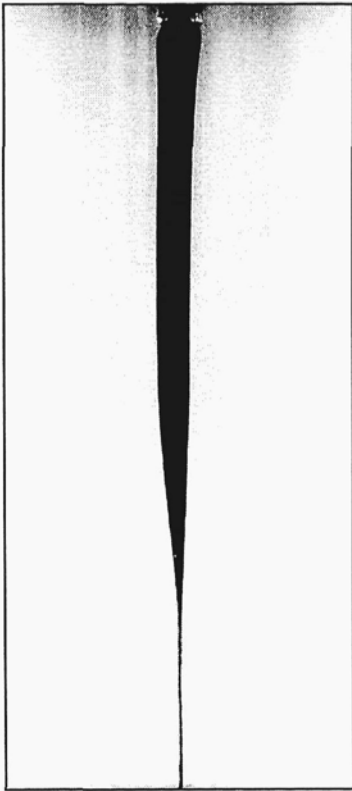


Figure 4.3a. Experiment number 1.

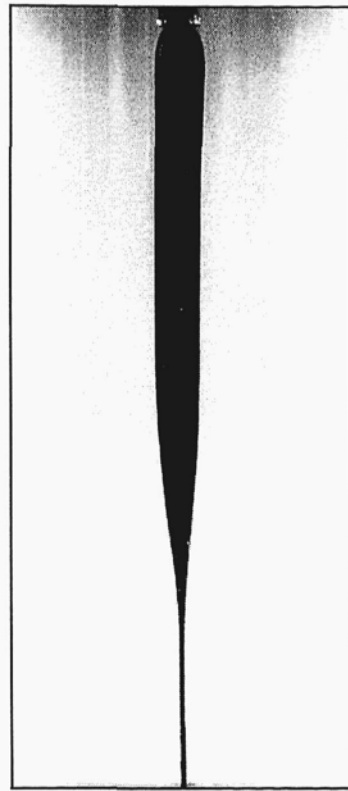


Figure 4.3b. Experiment number 2.

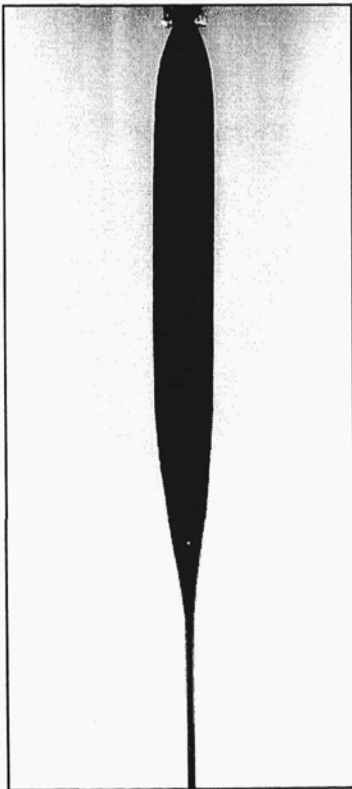


Figure 4.3c. Experiment number 3.

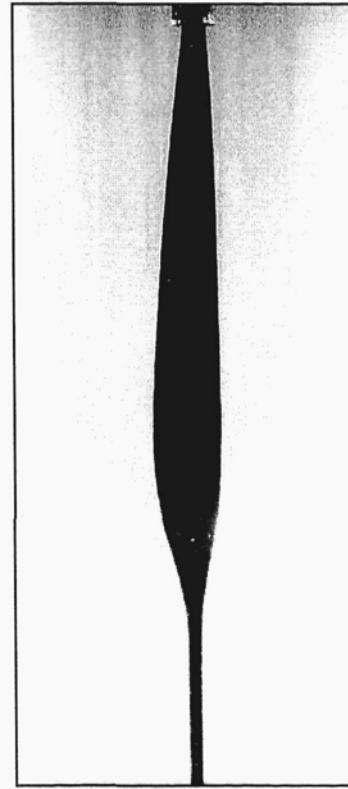


Figure 4.3d. Experiment number 4.

Mixing of liquids of equal viscosities and densities.

The numerical calculations were performed under assumption that red-ox reaction of iodine with sodium thiosulfate:



is instantaneous; Wilson [70] reported the reaction rate constant equal to $3 \cdot 10^7$ dm³/mol/s in pure water, Saito et al. [32] found $k=5.8 \cdot 10^8$ dm³/mol/s in aqueous solutions of corn syrup. It was additionally assumed that coefficients of molecular diffusion for both reactants are the same and equal to 10^{-10} m²/s; Saito et al. [32] reports values between 10^{-10} m²/s and 10^{-11} m²/s for **D** in aqueous solutions of corn syrup ($0.1 \text{ Pa}\cdot\text{s} < \mu < 1 \text{ Pa}\cdot\text{s}$).

Numerical integration of equations of motion and continuity for steady-state, axisymmetric flow:

$$u \cdot \frac{\partial u}{\partial r} + w \cdot \frac{\partial u}{\partial z} = -\frac{1}{\rho} \cdot \frac{\partial p}{\partial r} + \nu \cdot \left[\frac{\partial}{\partial r} \left(\frac{1}{r} \cdot \frac{\partial(r \cdot u)}{\partial r} \right) + \frac{\partial^2 u}{\partial z^2} \right], \quad (4.2a)$$

$$u \cdot \frac{\partial w}{\partial r} + w \cdot \frac{\partial w}{\partial z} = -\frac{1}{\rho} \cdot \frac{\partial p}{\partial z} + \nu \cdot \left[\frac{1}{r} \cdot \frac{\partial}{\partial r} \left(r \cdot \frac{\partial w}{\partial r} \right) + \frac{\partial^2 w}{\partial z^2} \right], \quad (4.2b)$$

$$\frac{1}{r} \cdot \frac{\partial(r \cdot u)}{\partial r} + \frac{\partial w}{\partial z} = 0 \quad (4.3)$$

and material balance equation

$$u \cdot \frac{\partial c}{\partial r} + w \cdot \frac{\partial c}{\partial z} = D \cdot \left[\frac{1}{r} \cdot \frac{\partial}{\partial r} \left(r \cdot \frac{\partial c}{\partial r} \right) + \frac{\partial^2 c}{\partial z^2} \right] \quad (4.4)$$

with boundary conditions:

$$\text{– at mixer axis } (r=0) \quad u=0, \quad \frac{\partial c}{\partial r}=0, \quad (4.5a)$$

$$\text{– at mixer walls} \quad u=w=0, \quad \nabla(c) \cdot \hat{n}=0, \quad (4.5b)$$

$$\text{– at central inlet } (0 \leq r \leq r_1) \quad u=0, \quad w=2 \cdot \bar{w}_1 \cdot \left[1 - (r/r_1)^2 \right], \quad c=c_{A0}, \quad (4.5c)$$

$$\text{– at annular inlet } (r_1 \leq r \leq r_2) \quad u=0, \quad c=-c_{B0},$$

$$w=2 \cdot \bar{w}_2 \cdot \left[1 - \left(\frac{r}{r_2} \right)^2 + \frac{1 - (r_1/r_2)^2}{\ln(r_2/r_1)} \cdot \ln \left(\frac{r}{r_2} \right) \right] / \left[1 + \left(\frac{r_1}{r_2} \right)^2 - \frac{1 - (r_1/r_2)^2}{\ln(r_2/r_1)} \right] \quad (4.5d)$$

were solved by Fluids Dynamics Analysis Package FIDAP6 using the finite element method.

After simulations concentration profiles of species reacting instantaneously were obtained from the following formulas [66]:

$$c_A = \frac{|c| + c}{2}, \quad (4.6a)$$

$$c_B = \frac{|c| - c}{2}, \quad (4.6b)$$

where **A** and **B** are iodine and sodium thiosulfate respectively.

Figure 4.4 shows the calculated (a) and measured shapes (b) of the coloured iodine zone. The distribution of the elongation rate ($\partial w / \partial z$) along the mixer axis, plotted in figure 4.4c is also well correlated with the observed shape of the core liquid. The negative and positive elongation rates are related to expansion and contraction of the core liquid respectively.

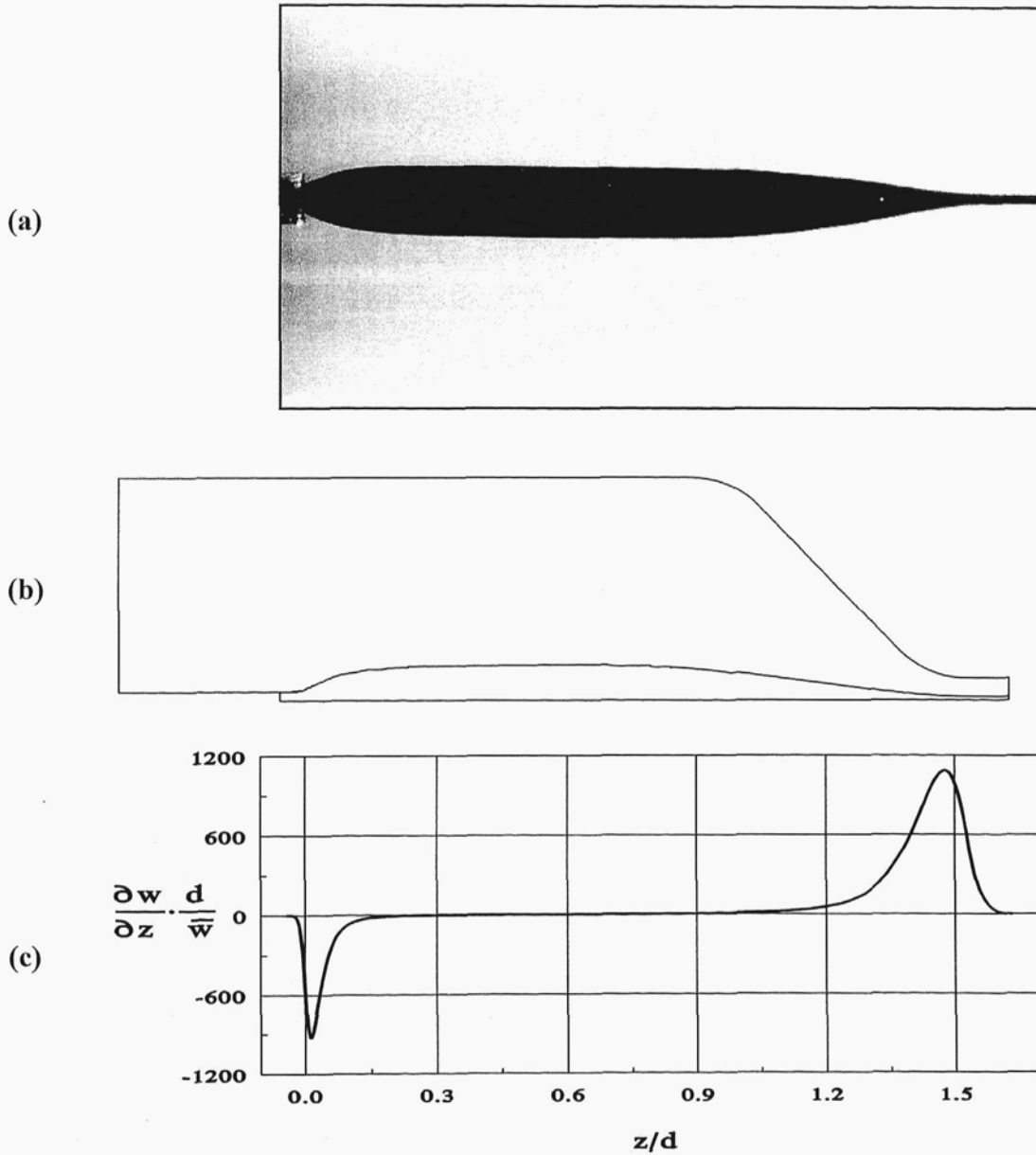


Figure 4.4. Shape of the iodine stream (exp.no.3): experimental (a), calculated (b), elongation rate at $r=0$ (c); $d=2 r_2$, $\bar{w}=4 (Q_1+Q_2)/(\pi d^2)$.